

Colloid-Polymer Interplay in the Local Longitudinal Fluctuations of F-actin Solutions

Pablo Domínguez-García,¹ Jose R. Pinto,² Ana Akrap,³ and Sylvia Jeney³

¹*Dep. Física Interdisciplinar, Universidad Nacional de Educación a Distancia (UNED), Madrid, Spain**

²*Department of Biomedical Sciences, Florida State University College of Medicine, Florida, USA.*

³*Department of Physics, University of Fribourg, Fribourg, Switzerland*

(Dated: September 16, 2022)

We study the motion of single trapped microtracers immersed in F-actin solutions by optical trapping interferometry in order to clarify the observed variability of their anomalous power-law exponent. We obtain a local 7/8 exponent only for non-adsorbing polymer at low optical trapping forces, a value which decreases when increasing the trap stiffness. The velocity autocorrelation function confirms the complex interplay in the colloid-polymer system even under the influence of small external forces and shows an additional constant power-law exponent for the depleted particles.

Optical tweezers (OT) have been demonstrated as a revolutionary technique in soft matter, complex fluids and biophysics since Ashkin and co-workers published their seminal paper [1]. Using focused beams of laser light, OT allow to trap and control tracer micrometer-sized particles suspended in a complex fluid, and, therefore, the study of such fluid on biologically relevant scales. Since the position fluctuations of the trapped tracer depend on the properties of the surrounding medium, the viscoelastic properties of the fluid can be inferred by microrheology [2]. However, even very small forces applied to the fluid (usually a polymeric suspension) may affect the mechanical properties of the bead's surroundings [3, 4]. This drawback becomes interesting when we focus on the interaction between the colloidal particle and the polymers which defines the fluid behavior. The optical force affects the colloid-polymer system, already complex because of the interaction with the biomaterial, the compressibility of the matrix network, and the polymer adsorption and depletion effects near the colloid surface [5–8]. In practice, the understanding of colloid-polymer interactions is important for their role in industrial applications, from food technologies to personal care products [9].

As a model case of semiflexible polymer, filamentous actin (F-actin) has been object of intense investigations during the past three decades in the context of biophysics and microrheology. This polymer is the most abundant protein of the cytoskeleton in eukaryotic cells and determine their mechanical properties [10], being also involved in different bioprocesses, remarkably muscle contraction [11]. F-actin has a diameter of $d \sim 7$ nm [12] and an average contour length $l \sim 20$ μ m [13], persistence length $l_p \sim 17$ μ m [14] (in the range 9–20 μ m depending on preparation [15]), and mesh size $\xi(\mu\text{m}) = 0.3/\sqrt{c_A}$, where c_A is the concentration of actin in mg/ml [16]. The length scale relevant for elastically active contacts is the entanglement length, l_e , which is the characteristic scale where an individual filament is sterically hindered because of other polymers nearby [17]. This length is a phenomenological parameter difficult to measure, but for physiological values of F-actin, it is reported to be

$l_e \sim 1 - 2$ μ m [18–20]. For $c_A = 1$ mg/ml, these semiflexible polymers [21] verify $d \ll \xi < l_p \sim l$. If we take into account the optically-trapped tracer, its radius a has to be smaller than the mesh size, so that its motion reflects the mechanical properties of the surrounding medium. Then, for measuring F-actin networks, we need $d \ll \xi < a < l_e < l_p \sim l$. To explore these conditions, here we use two tracer sizes: $a = 0.99$ μ m, satisfying the condition $a < l_e$; and $a = 1.47$ μ m, with $a \sim l_e$, which does not match the required condition. For the former case, we use chemically-active polystyrene (PS) particles (Sigma-Aldrich), but coated with BSA (bovine serum albumin, Sigma-Aldrich), blocking polymer surface absorption to explore their motion in the presence of a depletion layer. For the latter, we employ chemically inert melamine resin particles (Microparticles, GmbH).

The inspection of the motion of those particles inside the polymeric network for these two limit-cases will provide an insight of the complex colloid-polymer interplay, specially in the presence of external optical forces. In this Letter, we focus on the power-law behavior of F-actin solutions, but some reported exponents in the literature (see extended discussion in the accompanying paper [22]) deviate from the expected results for semiflexible polymers. We clarify this aspect by studying the local actin longitudinal fluctuations, which we find to depend on the colloid size/polymer length scales, and on the external forces/bead's surface characteristics.

The motion of single-tracers is used to deduce the mechanical properties of the fluid. One-particle (1P) microrheology provides the fluid viscoelasticity on the microscale, similar to the tracer's size, i.e., microrheology depends of the length scales in the system [23], as opposed to bulk rheology [24]. To overcome the limitations of 1P microrheology, two-particle (2P) microrheology [25, 26] detects the fluctuations at large length scales, matching bulk rheology as a result [27]. F-actin solutions are a classic example of substantial differences between micro- and macrorheology results, but a correct characterization of the involved length scales can clarify some of the discrepancies in other viscoelastic fluids [28]. The advantage of classical 1P microrheology relies on its po-

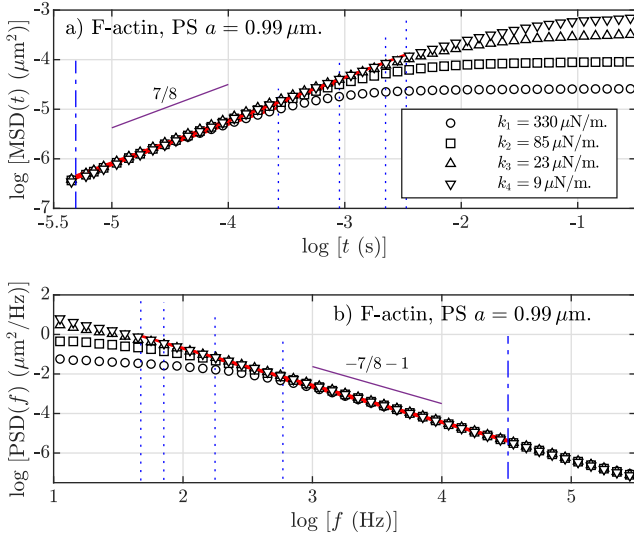


FIG. 1. (Color online) a) One dimensional mean-squared displacement (MSD) and b) Power spectral density (PSD) for 1 mg/ml F-actin solution for an optically trapped polystyrene (PS) BSA-added tracer with $a = 0.99 \mu\text{m}$. All the experimental data have been blocked in 10 bins per decade. Errors are negligible, not plotted for clarity. Trapping forces are indicated in the legend. Regression lines (—) are calculated under the limits defined by the blue dashed lines: top (.....) and lower limits (---) for the MSD (a), inversely for the PSD (b). The purple line (—) is a guide for the eye indicating the power-law exponent $\alpha = 7/8$.

tential capacity for isolating the local contribution to the fluctuations in the scale of the tracer bead, therefore, allows to investigate the polymer dynamics in the biological scale.

In this work, the motion of single optically-trapped tracer beads is measured using optical trapping interferometry (OTI), which consists of an optical trap combined with an interferometric position detector, allowing measurements of the Brownian position fluctuations of the microbead with nanometric resolution in the microsecond range [29]. The trajectories were collected during 100 s at a sampling rate of 1 MHz, corresponding to 10^8 data points per measurement. In an accompanying paper [22], we provide further information about the experimental set-up, materials, and methods.

Fig. 1 plots the one-dimensional mean-squared displacement, $\text{MSD}(t) \equiv \langle (x(t) - x(0))^2 \rangle$, and the power spectral density, $\text{PSD}(f)$, for a micron-sized PS BSA-added bead immersed in a F-actin solution [30] under four different trap stiffnesses, k_i . The MSD reaches a plateau at higher times because of elastic forces from the trap and the fluid itself. At intermediate and short-time values, it verifies an anomalous power-law behavior $\text{MSD}(t) \sim t^\alpha$ with $\alpha < 1$, before the influence of hydrodynamic and inertia effects. The behavior of the PSD is analogous but in the frequency space, showing a

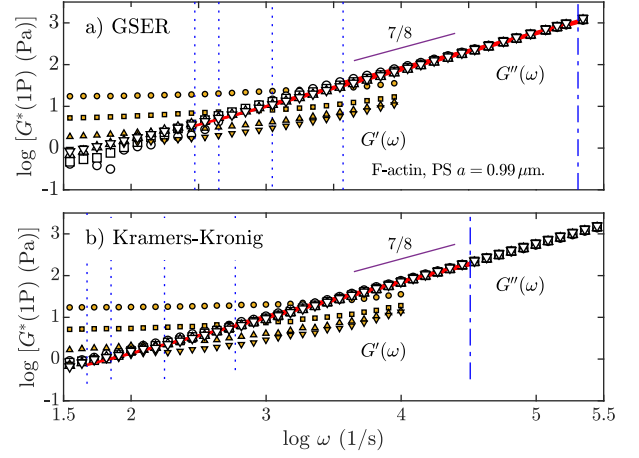


FIG. 2. (Color online) Real (storage modulus, $G'(\omega)$, smaller points) and imaginary (loss modulus, $G''(\omega)$) parts of the complex modulus, $G^*(\omega)$, for an optically trapped polystyrene (PS) BSA-added tracer with $a = 0.99 \mu\text{m}$ in 1 mg/ml F-actin solution. a) Obtained by means of the GSER and the MSD, or b) through the Kramers-Kronig expression. Symbols and lines are the same as in Fig. 1.

$\text{PSD}(f) \sim f^{-\alpha-1}$ decay.

Fig. 2 shows the complex modulus, $G^*(\omega) = G'(\omega) + iG''(\omega)$, where G' is the storage or elastic modulus and G'' is the loss modulus. These quantities are obtained by means of standard microrheological methods, i.e., by means of the generalized Stokes-Einstein relation (GSER) concurrent with Mason's approximation [31, 32], shown in Fig. 2a), and through the Kramers-Kronig integrals, Fig. 2b). The loss modulus calculated by both methods follows a power-law behavior $G''(\omega) \sim \omega^\alpha$. In this study, by analyzing the power-law behavior of the functions $\text{MSD}(t)$, $\text{PSD}(f)$ and $G''(\omega)$, we systematically calculate α values for an appreciable collection of measurements. In the case of PS particles, we obtain results compatible with an exponent $\alpha \approx 7/8$. However, according to theory, bulk rheology, and bulk-compatible microrheology, the exponent α is equal to $3/4$ for this kind of polymeric networks [33]. On the other hand, an exponent $\alpha = 7/8$ is obtained in F-actin solutions when adding myosin [34] and also appears in some experiments similar to the reported in this Letter [35]. The origin of this exponent value relies on the longitudinal response provoked by a local microperturbation in the polymer generated by the tracers. The finite propagation of the tension along the filament generates a more rapid variation in the mean-squared displacement through a $t^{7/8}$ growth at low time-scales [36].

Semiflexible polymers form entangled networks at very low concentrations and their units are sterically hindered by other filaments at the entanglement length, which should generate a constant value for the elastic modulus, $G'(\omega)$, over an extended range of frequencies [24].

TABLE I. Averaged power-law exponents polystyrene (PS) BSA-added tracers ($a = 0.99 \mu\text{m}$ with optical stiffness $k = 9 \pm 4 \mu\text{N/m}$). The parentheses in the numbers are concise notation for the numerical value of the standard uncertainty. F-actin/Tm and F-actin/Tm/Tn experiments were performed in the presence of Ca^{2+} [22].

Material	$\langle\alpha_{\text{MSD}}\rangle$	$\langle\alpha_{\text{PSD}}\rangle$	$\langle\alpha_{\text{GSER}}\rangle$	$\langle\alpha_{\text{KK}}\rangle$	$\langle\beta_{\text{VAF}}\rangle$
Actin	0.873(11)	0.869(13)	0.883(9)	0.857(13)	0.90(4)
A.Tm.	0.879(2)	0.875(3)	0.888(2)	0.862(3)	0.884(12)
A.Tm.Tn.	0.888(3)	0.877(4)	0.887(2)	0.858(7)	0.91(2)

In Fig. 2, we observe constant values for $G'(\omega)$ even at the lowest optical force, but this effect is not detected in bulk rheology, where $G'(\omega)$ grows with frequency and the elastic plateau only appears at very low frequencies. The increase of the elastic modulus with frequency occurs because of the fluctuations of the filaments over their persistence length, on a scale of tens of microns. On the contrary, if we measure locally, on the order of microns, the relevant scale lengths are the mesh size and, especially, the entanglement length. Additionally, we check the exposed local mechanical properties of F-actin by adding skeletal muscle tropomyosin (Tm) alone, and Tm and troponin (Tn). Tm is a coiled-coil protein, which, together with actin and Tn, constitutes the thin filament. The coupling of Tm/Tn complex to actin, regulated by the presence of Ca^{2+} [37], allows myosin and actin interaction and thus muscle contraction. Mechanically, Tm/Tn complex tends to stabilize the filament structure and increases its stiffness, but without major modifications in the network structure [38]. Our analysis of the motion of PS particles immersed in F-actin/Tm and F-actin/Tm/Tn complexes, always in the presence of calcium, returns very similar curves to the ones shown in Fig. 1 and 2, providing analogous results when averaging α values (see Table I and details in the accompanying paper [22]).

The general picture described until now changes when we focus on the influence of the optical forces and when we repeat the same experiments using chemically-inert melamine resin particles. Fig. 3 shows how our experiments using micro-sized PS BSA-added particles return $\alpha \approx 7/8$ for low optical forces, but, when we increase the trap stiffnesses, the exponent slightly decreases. Such an effect may be attributed to the effective increase of particle size, because of surface adsorption already improved by the attractive optical force affecting the polymers, but this effect is blocked by BSA. In this case, the filamentous polymers are not attached to the bead, and a less dense network is formed around the particle, generating a polymer-poor depletion zone because of the entropy loss of the molecules near the bead surface. Experimentally, it has already been observed that the increase of the depletion agent concentration in actin solutions decreases

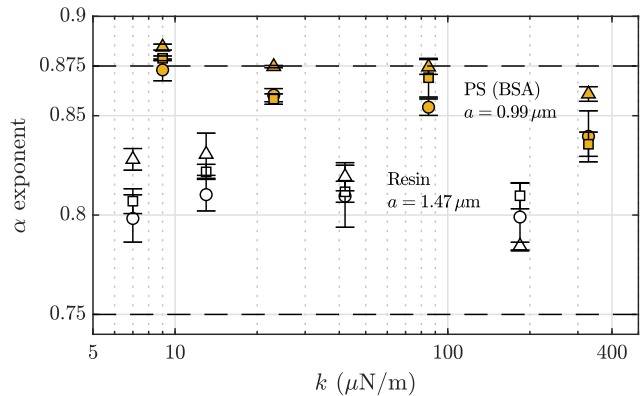


FIG. 3. Dependence of the averaged values of the local power-law exponent α with applied optical trap stiffness for polystyrene (PS) BSA-added (F-actin: \bullet , F-actin/Tm: \blacksquare , and F-actin/Tm/Tn: \blacktriangle) and melamine resin tracers (F-actin: \circ , F-actin/Tm: \square , and F-actin/Tm/Tn: \triangle). Horizontal bar errors are not included for clarity. Dashed lines (---) are a guide for the eye indicating exponents $\alpha = 7/8$ and $3/4$.

the exponent of the power-law behavior in the complex modulus [39]. According to that result, it follows that the optical forces are acting like an effective depletion agent.

On the other hand, the resin particles give $\alpha \approx 0.81$ with no appreciable dependency with the optical trap strength, confirming that these beads have no surface-related effects, and also verifying the importance of their particular size, relative to the fluid's entanglement length ($a \sim l_e$), when we measure the local mechanical properties, providing an intermediate exponent between $7/8$ and the expected $3/4$. In relation to the influence of Tm/Tn, the obtained α values are very similar to F-actin alone, but a small increase in the averaged values can be observed in Fig. 3. If we visualize the whole data without averaging, we observe that α values are less dispersed when adding Tm or Tm/Tn (results detailed in Ref. [22]). This observation agrees with a stabilization of the filament structure by Tm/Tn, even when measured locally.

Finally, we study the velocity autocorrelation function defined as $\text{VAF}(t) \equiv \langle v(t)v(0) \rangle$, where v is the velocity of the particle. Fig. 4a) plots this function in absolute values ($|\text{VAF}(t)|$) for PS tracers, showing a dependence of the numeric values with the applied optical force, where the data with the strongest optical force on top and the weakest at the bottom. Such an effect does not appear for resin tracers, as it can be seen in Fig. 4b). The VAF is related to the dissipation of the particle's motion by its interaction with the surrounding viscoelastic network. This observation confirms the interpretation that the optical forces are acting like a depletion agent for the non-adsorbing polymer PS tracers, increasing the low-

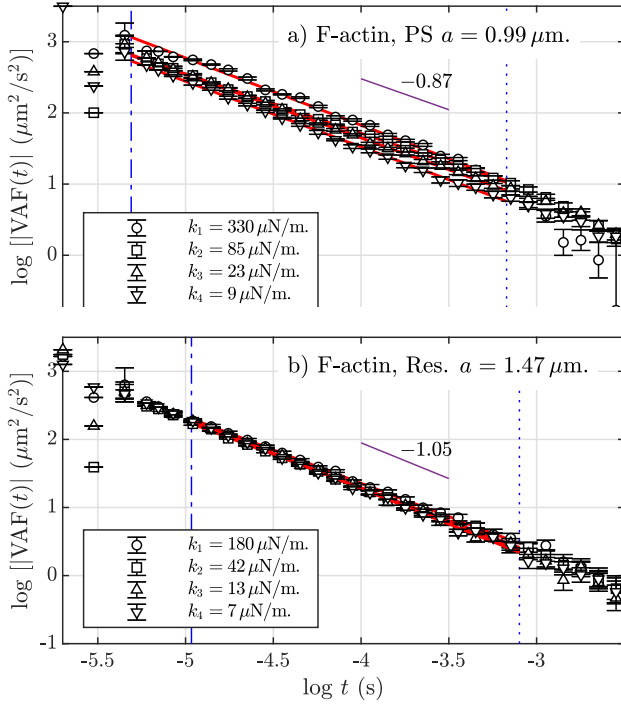


FIG. 4. (Color online) Absolute values of the velocity auto-correlation function, $|VAF|$ at 1 mg/ml F-actin solution for a) polystyrene (PS) BSA microparticle with $a = 0.99 \mu\text{m}$. and b) melamine resin with $a = 1.47 \mu\text{m}$. The errors are calculated by the blocking method. Data points for the different trap stiffnesses are indicated in the legends. Regression lines (—) are calculated under the limits defined by the blue dashed lines: top (.....) and lower limits (---). The purple lines (—) is a guide for the eye indicating the averaged power-law exponent β in each case.).

viscosity region around the particles. Regarding its multiple power-law behavior, it is known that the VAF shows a minimum in the first zero-crossing value, related to the interplay between the optical trapping and the hydrodynamics of the fluid. In Newtonian fluids, before that minimum, this function follows an algebraic power-law rather than an exponential tail $|VAF|(t) \sim t^{-3/2}$, known as the “long-time tail” [40]. A second zero-crossing appears at higher time scales, before a power-law decay in the form of $\sim t^{-7/2}$, but its observation is very limited by the initial noise floor of the experimental set-up. In Fig. 4, we observe a third power-law behavior, $|VAF|(t) \sim t^{-\beta}$, for an intermediate time-scale. We obtain two different exponents, averaged for all k values: $\beta = 0.870(6)$ for PS particles, Fig. 4a), and $\beta = 1.050(3)$ for resin tracers, Fig. 4b). A similar value to the resin beads exponent has been previously observed in actin solutions ($\beta = 0.97$) [41]. Remarkably, these exponents do not depend on the applied optical forces, only on the type of tracer.

The exponent value $\beta \sim 1$ for the resin tracers can be deduced from a power-law fluid $\text{MSD}(t) \sim t^\alpha$ by mak-

ing its second derivative, so $VAF(t) \sim t^{-\beta=\alpha-2}$. Therefore, if $\alpha = 7/8$, then $\beta \approx 1.1$. More accurately, if we use the published data from a complete phenomenological power-law model which includes inertial and hydrodynamic effects at short-times and optical trapping at long times [42], we obtain an estimated $\beta = 1.08$ for $\alpha = 0.81$, matching our experimental result. However, to our knowledge, the exponent $\beta < 1$ for depleted PS particles has not been previously observed. Its physical interpretation is not clear, but the effects of the depletion layer are indeed more complex than expected, something confirmed by numerical studies of mean-field theory, which show that the depletion thickness and curvature effects depend on the interplay between the persistence and correlation polymer characteristic lengths [43]. Unfortunately, there is a lack of numerical and theoretical studies of the behavior of semiflexible polymers near spherical particles.

The results summarized in this Letter clarify the variability of power-law exponents in F-actin solutions reported in the literature by measuring the local longitudinal fluctuations of actin polymeric filaments, under the condition of a previous knowledge of the basic characteristic of the fluid. By analyzing the anomalous diffusion of microtracers immersed in these networks, we have observed a dependence of the power-law α exponents and the velocity autocorrelation function with the applied external forces, related to the interplay between the depletion layer surrounding the colloid and the external optical trap. The understanding of the mechanical response of these biopolymeric networks in the microscale may expand the knowledge of the microscopical origins of their rheology and our capacity to emulate biological systems. A potential application for the observations contained in this Letter may be the ability to tune the depletion forces around colloidal particles by the application of lightly controlled external forces.

P.D.G acknowledges support aid by grant PID2020-117080RB-C54 funded by MCIN/AEI/10.13039/501100011033, J.R.P. from National Institutes of Health grant R01 HL128683, and A.A. funding from the Swiss National Science Foundation through project PP00P2_202661.

* pdominguez@fisfun.uned.es

- [1] A. Ashkin, J. M. Dziedzic, J. E. Bjorkholm, and S. Chu, *Opt. Letters* **11**, 288 (1986).
- [2] T. G. Mason and D. A. Weitz, *Phys. Rev. Lett.* **74**, 1250 (1995).
- [3] M. Tassieri, *Soft Matter* **11**, 5792 (2015).
- [4] P. Domínguez-García, L. Forró, and S. Jeney, *Appl. Phys. Lett.* **109**, 143702 (2016).
- [5] E. Donath, A. Krabi, M. Nirschl, V. M. Shilov, M. I. Zharkikh, and B. Vincent, *J. Chem. Soc., Faraday Trans.*

- 93**, 115 (1997).
- [6] D. T. Chen, E. R. Weeks, J. C. Crocker, M. F. Islam, R. Verma, J. Gruber, A. J. Levine, T. C. Lubensky, and A. G. Yodh, *Phys. Rev. Lett.* **90**, 108301 (2003).
 - [7] M. T. Valentine, Z. E. Perlman, M. L. Gardel, J. H. Shin, and P. Matsudaira, *Biophys. J.* **86**, 4004 (2004).
 - [8] J. He and J. X. Tang, *Phys. Rev. E* **83**, 041902 (2011).
 - [9] R. G. Larson, *The Structure and Rheology of Complex Fluids* (Oxford University Press, New York, 1999).
 - [10] G. Bao and S. Suresh, *Nat. Mater.* **2**, 715 (2003).
 - [11] S. Y. Bershitsky, A. K. Tsaturyan, O. N. Bershetskaya, G. I. Mashanov, P. Brown, R. Burns, and M. A. Ferenczi, *Nature* **388**, 186 (1997).
 - [12] E. H. Egelman, *J. Muscle Res. Cell Motil.* **6**, 129 (1985).
 - [13] S. Kaufmann, J. Käs, W. H. Goldmann, E. Sackmann, and G. Isenberg, *FEBS Letters* **314**, 203 (1992).
 - [14] A. Ott, M. Magnasco, A. Simon, and A. Libchaber, *Phys. Rev. E* **48**, R1642 (1993).
 - [15] H. Isambert, P. Venier, A. C. Maggs, A. Fattoum, R. Kassab, D. Pantaloni, and M. F. Carlier, *J Biol Chem.* **270**, 11437 (1995).
 - [16] C. F. Schmidt, M. Baermann, G. Isenberg, and E. Sackmann, *Macromolecules* **22**, 3638 (1989).
 - [17] F. C. MacKintosh, J. Käs, and P. A. Janmey, *Phys. Rev. Lett.* **75**, 4425 (1995).
 - [18] H. Isambert and A. C. Maggs, *Magnetohydrodynamics* **29**, 1036 (1996).
 - [19] A. Palmer, T. G. Mason, J. Xu, S. C. Kuo, and D. Wirtz, *Biophys. J.* **76**, 1063 (1999).
 - [20] K. M. Addas, C. F. Schmidt, and J. X. Tang, *Phys. Rev. E* **70**, 021503 (2004).
 - [21] If $l \sim l_p$, the network of semiflexible polymers is in the *highly entangled isotropic* regime, while if ξ and l_e are both much less than l_p , then the solution is in the *tightly entangled* regime. In this work, the terms network and solution are equivalent and describe a semidilute solution of uncrosslinked F-actin.
 - [22] P. Domínguez-García, J. R. Pinto, A. Akrap, and S. Jeney, “Micro-mechanical response of the f-actin/tropomyosin/troponin complex by optical trapping interferometry,” (2022).
 - [23] M. Atakhorrami, G. H. Koenderink, J. F. Palierne, F. C. MacKintosh, and C. F. Schmidt, *Phys. Rev. Lett.* **112**, 088101 (2014).
 - [24] M. L. Gardel, M. T. Valentine, J. C. Crocker, A. R. Bausch, and D. A. Weitz, *Phys. Rev. Lett.* **91**, 158302 (2003).
 - [25] A. J. Levine and T. C. Lubensky, *Phys. Rev. Lett.* **85**, 1774 (2000).
 - [26] J. C. Crocker, M. T. Valentine, E. R. Weeks, T. Gisler, P. D. Kaplan, A. G. Yodh, and D. A. Weitz, *Phys. Rev. Lett.* **85**, 888 (2000).
 - [27] Basically, 2P microrheology measures bulk viscoelasticity, without the influence of the local environment, because of the propagation through the medium of the interparticle position correlations generated by elastic and hydrodynamics iterations.
 - [28] M. Buchanan, M. Atakhorrami, J. F. Palierne, and C. F. Schmidt, *Macromolecules* **38**, 8840–8844 (2005).
 - [29] T. Franosch, M. Grimm, M. Belushkin, F. M. Mor, G. Foffi, L. Forró, and S. Jeney, *Nature (London)* **478**, 85 (2011).
 - [30] Phalloidin-stabilized (1 mM) F-actin (23.8 μ M) has been polymerized from monomeric actin from rabbit skeletal muscle according to standard recipe [44] See further details in the accompanying paper [22].
 - [31] T. G. Mason, K. Ganesan, J. H. van Zanten, D. Wirtz, and S. C. Kuo, *Phys. Rev. Lett.* **79**, 3282 (1997).
 - [32] T. G. Mason, *Rheol. Acta* **39**, 371 (2000).
 - [33] F. Gittes and F. C. MacKintosh, *Phys. Rev. E* **58**, R1241 (1998).
 - [34] L. Le Goff, F. Amblard, and E. M. Furst, *Phys. Rev. Lett.* **88**, 018101 (2001).
 - [35] See for example: Chae and Furst, *Langmuir*, 3084 (2005); Koenderink *et al.*, *Phys. Rev. Lett.* **96**, 138307 (2006); Atakhorrami *et al.*, *Phys. Rev. E* **77**, 061508 (2008); Tassieri *et al.*: *Biophys. J.* **94**, 2170 (2008), and *New J. Phys.* **14** (2012); Grebenkov *et al.*, *Phys. Rev. E* **88**, 040701 (2013); and Ref. [23].
 - [36] R. Everaers, F. Jülicher, A. Ajdari, and A. C. Maggs, *Phys. Rev. Lett.* **82**, 3717 (1999).
 - [37] S. Ebashi, T. Wakabayashi, and F. Ebashi, *J. Biomech.* **69**, 441 (1971).
 - [38] R. Götter, G. K., E. Frey, B. M., and E. Sackmann, *Magnetohydrodynamics* **29**, 30 (1996).
 - [39] R. Tharmann, M. M. A. E. Claessens, and A. R. Bausch, *Biophys. J.* **90**, 2622 (2006).
 - [40] B. J. Alder and T. E. Wainwright, *Phys. Rev. A* **1**, 18 (1970).
 - [41] J. Xu, W. H. Schwarz, J. A. Käs, T. P. Stossel, P. A. Janmey, and T. D. Pollard, *Biophys. J.* **74**, 2731 (1998).
 - [42] D. S. Grebenkov and M. Vahabi, *Phys. Rev. E* **89**, 012130 (2014).
 - [43] V. Ganesan, L. Khounlavong, and V. Pryamitsyn, *Phys. Rev. E* **78**, 051804 (2008).
 - [44] J. D. Pardee and S. J. A, *Methods Enzymol.* **85**, 164 (1982).